Sonoporation increases therapeutic efficacy of inducible and constitutive BMP2/7 *in vivo* gene delivery

G. A. Feichtinger[1], A. T. Hofmann[1], P. Slezak[1], S. Schuetzenberger[1], M. Kaipel[1], E. Schwartz[2], A. Neef[3], N. Nomikou[5], T. Nau[1], M. van Griensven[1,4], A. P. McHale[5], H. Redl[1]

[1] Ludwig Boltzmann Institute for Experimental and Clinical Traumatology, AUVA Research Center, Austrian Cluster for Tissue Regeneration, European Institute of Excellence on Tissue Engineering and Regenerative Medicine Research (Expertissues EEIG), Vienna-Branch, Vienna, Austria

[2] Computational Image Analysis and Radiology Laboratory, Department of Radiology, Medical University of Vienna, Vienna, Austria

[3] Organic Chemistry Institute, University of Zurich, Zurich, Switzerland

[4] Experimental Trauma Surgery, Klinikum Rechts der Isar, Technical University Munich, Munich, Germany

[5] School of Pharmacy and Pharmaceutical Science, University of Ulster, Coleraine, United Kingdom

Correspondence should be adressed to G. A. Feichtinger

email: georg.feichtinger@trauma.lbg.ac.at

Donaueschingenstrasse 13

A-1200-Vienna, Austria

Phone: +43133110793

Fax: +43133110460

Short title: BMP2/7 sonoporation for bone regeneration

ABSTRACT

An ideal novel treatment for bone defects should provide regeneration without autologous or allogenous grafting, exogenous cells, growth factors or biomaterials while ensuring spatial and temporal control as well as safety. Therefore, a novel osteoinductive non-viral *in vivo* gene therapy approach using sonoporation was investigated in ectopic and orthotopic models. Constitutive or regulated doxycycline-inducible bone morphogenetic protein 2 and 7 co-expression plasmids were repeatedly applied for 5 days. Ectopic and orthotopic gene transfer efficacy was monitored by co-application of a luciferase plasmid and bioluminescence imaging. Orthotopic plasmid DNA distrubution was investigated using a novel plasmid labeling method. Luciferase imaging demonstrated an increased trend (61% vs 100%) of gene transfer efficacy and μCT evaluation showed significantly enhanced frequency of ectopic bone formation for sonoporation compared to passive gene delivery (46% vs 100%) dependent on applied ultrasound power. Bone formation by the inducible system (83%) was stringently controlled by doxycycline *in vivo* and no ectopic bone formation was observed without induction or with passive gene transfer without sonoporation. Orthotopic evaluation in a rat femur segmental defect model demonstrated an increased trend of gene transfer efficacy using sonoporation. Investigation of DNA distribution demonstrated extensive binding of plasmid DNA to bone tissue. Sonoporated animals displayed a potentially increased union rate (33%) without extensive callus formation or heterotopic ossification. We conclude that sonoporation of BMP2/7 co-expression plasmids is a feasible, minimally invasive method for osteoinduction & improvement of bone regeneration by gene delivery being superior to passive gene delivery.

Keywords: Sonoporation, non-viral, gene therapy, heterodimer, bone morphogenetic protein, BMP2/7, TetON, inducible, ectopic, orthotopic

INTRODUCTION

Traumatic fractures can lead to defects of critical size that can fail to regenerate completely, depending on the fracture site and general clinical situation of the patient (Stannard *et al*., 2007). These non-union fractures, also termed pseudoarthroses, are characterized by a failure to heal within 8-9 months (Stannard *et al*., 2007). Such a situation represents a major clinical challenge, which is still not addressed adequately by conventional treatment. Autologous bone grafting from the iliac crest can provide satisfying regenerative outcome, although at the cost of an invasive procedure requiring surgical intervention causing donor site morbidity (Jones CB, 2005; MK Sen, 2007). Other experimental treatment modalities include combinations of autologous stem cell treatment, biomaterials and growth factors (Axelrad *et al*., 2007; Bruder *et al*., 1998; Kanakaris and Giannoudis, 2008; Schmidmaier *et al*., 2008). Therapies that rely on stem cell treatment require invasive sampling and *in vitro* expansion of these cells prior to implantation, which again can lead to donor site morbidity and furthermore require expensive GMP facilities for safe cell enrichment and expansion (Verbeek, 2012). Furthermore, these procedures hold the inherent drawback of currently failing to be applied in a minimally invasive one-step approach. Recombinant growth factors on the other hand, are expensive in production (Vaibhav *et al*., 2007) and interestingly need to be applied in potentially dangerous supraphysiological doses (Gamradt SC, 2004), which can lead to adverse effects such as heterotopic ossification (Benglis *et al*., 2008) or immune responses (Hwang *et al*., 2009). A novel therapeutic approach should therefore enable a cost-effective, efficient and minimally invasive treatment of non-union fractures. It should preferentially be applied in a one-step procedure without the need for autologous or allogeneic implantation material. Several studies have demonstrated the feasibility of transient gene therapies for osteoinduction either through *ex vivo* (Gamradt SC, 2004) or *in vivo* viral (Bleiziffer *et al*., 2007) or non-viral gene transfer (Bleiziffer *et al*., 2007; Luo *et al*., 2005). The main advantage of this approach is that endogenous cells are forced to express an osteoinductive factor *in situ* directly at the fracture site, leading to correct post-translational modifications and conformation of the factor, thereby mediating higher bioactivity at lower concentrations compared to application of recombinant factors (Brooks, 2006). Since non-viral *in situ* gene transfer has a much better safety profile than viral modalities, it was selected as gene transfer modality within this study. Ultrasound mediated gene transfer (sonoporation), a relatively novel non-viral strategy that relies on neutral microbubble contrast agent mediated cell permeabilisation *in situ* to trigger

uptake of plasmid DNA (Li *et al*., 2009; S Mehier-Humbert, 2005), appears to be superior in terms of reduced invasiveness and clinical translation as compared to other non-viral methods such as electroporation (Cemazar *et al*., 2006). In order to compensate for lower efficacy of this non-viral gene transfer method, a highly osteoinductive co-expression strategy for bone morphogenetic protein (BMP) 2 and 7 (BMP2/7), which has been shown to potently mediate osteogenic differentiation *in vitro* (Kawai *et al*., 2006) and *in vivo* (Kawai *et al*., 2006; Zhao *et al*., 2005), was selected to be investigated for its regenerative potential in a femur non-union model in rats. The work presented herein is aimed at demonstrating the feasibility of an ultrasound mediated ("sonoporation") constitutive or regulated, doxycycline inducible BMP2/7 co-expression strategy for bone regeneration. This approach for enhanced fracture regeneration is solely relying on minimally invasive injection of a BMP2/7 co-expression plasmid DNA/microbubble mixture in conjunction with a transcutaneously applied ultrasound trigger to mediate deep within tissue *in vivo* non-viral transient gene transfer.

MATERIALS AND METHODS

Animals

The animal protocol review board of the City Government of Vienna, Austria approved all experimental procedures in accordance with Austrian law and the Guide for the Care and Use of Laboratory Animals as defined by the National Institute of Health. Female Hsd:Athymic Nude-Foxn1^{nu} nude mice (n=36) (Harlan Laboratories, Bresso, Italy) of approximately 12 weeks age weighing approx. 30g were used for ectopic testing in this study.

Male Sprague-Dawley rats (n=43) (Charles River, Wilmington, MA, US) weighing approx. 450g were used for orthotopic testing in this study.

Plasmids

The inducible and constitutive single-vector BMP2/7 co-expression plasmids, pTetON-BMP2/7 and pVAX1-BMP2/7- (Figure S1), are described elsewhere (Feichtinger *et al*. 2013, under review). Briefly, the constitutive pVAX1-BMP2/7- system was created by using a multi-expression cassette strategy with separate CMV-promoter driven BMP2 and BMP7 expression cassettes in divergent orientation on the FDA DNA vaccine guideline compliant plasmid backbone of pVAX1 (Life Technologies, Palo Alto, CA, US). The single-vector TetON inducible BMP2/7 co-expression system pTetON-BMP2/7 was derived from the Tet-regulated co-expression system pTREtight-BI (Takara Bio Europe/Clontech, Saint-Germain-en-Laye, France) by cloning BMP2 and BMP7 cDNAs into the multiple cloning sites and additionally transferring the entire Tet-transactivator expression cassette from pTetON-Advanced (Takara Bio Europe/Clontech, Saint-Germain-en-Laye, France) to pTREtightBI, generating a TetON inducible expression plasmid with 3 transcriptional entities. All plasmid preps were carried out using Endo-free plasmid Maxi or Giga kits (Qiagen, Hilden, Germany) or plasmids were produced as endo-free preps by Plasmid Factory (Bielefeld, Germany).

Sonoporation protocols

A SP100 Sonoporator (Sonidel Ltd, Dublin, Ireland) emitting 1MHz ultrasound was employed for sonoporative gene transfer in this study. The columnar beam was set at different Watt/cm^2 spatial average temporal peak settings with an effective radiating area of 0.8 cm^2 at a pulse frequency of 100Hz/100% duty cycle.

2 Watt/cm^2 treatment protocol: This protocol was a modified protocol derived from the ultrasound parameters applied in previous studies by Li *et al*. (Li *et al*., 2009). Daily treatment, which was repeated for 5 days consisted of application of 2 Watt/cm^2 1MHz ultrasound at a duty cycle of 25% for 3 minutes after injection of a plasmid DNA/microbubble contrast agent mixture. Total energy delivered to the target site per daily treatment was 90 Joule/cm^2.

4 Watt/cm^2 treatment protocol: This protocol was a modified protocol derived from Osawa *et al*. (Osawa *et al*., 2009). Daily treatment, repeated for 5 days, consisted of application of 4 Watt/cm^2 1MHz ultrasound at a duty cycle of 50% for 1min followed by a pause of 1min to prevent tissue overheating and was repeated for a total of 5 times (5x 1min treatment at 1 min intervals). Total energy delivered to the target site per day was 600 Joule/cm^2.

Animals were placed on a neoprene adsorber pad (Sonidel Ltd, Dublin, Ireland) with ultrasound contact gel (Aquasonic 100, Parker Laboratories Inc. Fairfield, New Jersey) to prevent reflection of ultrasound from the exit site back into the tissue and subsequent potential constructive interference with passing ultrasound, which could cause tissue overheating and damage.

Ectopic BMP2/7 sonoporation

Constitutive BMP2/7 co-expression in vivo

20μg constitutive co-expression plasmid pVAX1-BMP2/7- was co-delivered with 20μg of the internal luciferase control plasmid pCBR (Promega GmbH, Mannheim, Germany). Sonoporation was carried out using the SP100 device and neutral, lipid-based microbubbles (MB101, Sonidel Ltd, Dublin, Ireland) at a final concentration of 4x10^8/ml (50% v/v). 50μl of this plasmid-microbubble solution was injected into *m. gastrocnemius* in nude mice and immediately thereafter sonoporated. Anesthesia was initialized in an inhalation box provided with isoflurane (Forane®, Abbott Gesm.b.H., Vienna, Austria) (3 vol.% isoflurane-oxygen mixture) and maintained by inhalation of 1.5-2% isoflorane –oxygen mixture. This treatment was repeated for 5 subsequent days (total therapeutic DNA dose 100μg/animal; ~3.3mg/kg) using the same injection site. Sonoporation was carried out using either 2 Watt/cm^2 (25%

duty cycle) or 4 Watt/cm^2 (50% duty cycle) protocols in order to investigate the influence of ultrasound power settings on gene transfer efficacy. Hindlimbs were sonoporated for 1min 5 times using the described power settings. Gene transfer efficacies of sonoporated hindlimbs were compared to passive gene transfer in control hindlimbs without sonoporation. In order to investigate the potential competetive influence of an internal control plasmid on overall bone formation efficacy, 2 Watt/cm^2 sonoporations were additionally carried out without pCBR addition. 4 weeks after the surgery the mice were sacrificed in inhalation anaesthesia (see above) by an overdose of thiopentalsodium (Thiopental sandoz, Sandoz GmbH, Vienna, Austria) (120 mg/kg) by intracardiac injection and *gastrocnemius* muscles were explanted for histology.

Inducible BMP2/7 co-expression in vivo

The doxycycline inducible co-expression system for BMP2/7, TetON-BMP2/7, was sonoporated *in vivo* using the 2 Watt/cm^2 sonoporation protocol. The inducible systems were applied without an internal pCBR luciferase control plasmid. Controls for passive gene delivery were set up by intramuscular injection of the plasmids. Animals in the induction group received 2mg/day doxycycline in 300μl Ringer's solution intraperitoneally for 7days for induction of BMP2/7 co-expresssion after sonporative or passive gene transfer. Sonoporated control animals were not treated with doxycycline.

Orthotopic BMP2/7 sonoporation

Femur-defect model

Anaesthesia was induced via inhalation of 2% isoflurane and maintained through an intraperitoneal injection of a mixture of ketaminhydrochlorid, 110 mg/kg, (Ketamidor, Richter Pharma AG, Wels, Austria) and xylazin, 12 mg/kg (Rompun 2%, Bayer AG, Vienna, Austria). Preoperatively, the animals received a 2 ml liquid depot of Ringer's solution (Mayerhofer Pharmazeutika GmbH, Linz, Austria) mixed with 0.3 ml butafosan (Catosal, Bayer Health Care Austria GmbH, Vienna, Austria). Analgesia was provided via a daily subcutaneous injection of carprofen, 4 mg/kg (Rimadyl, Pfizer Corporation GmbH, Vienna, Austria) over the course of 4 days and a subcutaneous injection of buprenorphin, 0.05 mg/kg, every 12 hours during the first 2 days. During surgical procedure the rats were placed on a thermostatic plate in a lateral decubitus position. A lateral approach was used and the femur exposed. A straight, 4-hole titan plate (Stryker, Duisburg, Germany) was fixed onto the anterolateral surface of the femur using

four cortical 7mm titan screws (Synthes, Oberdorf, Switzerland). Subsequently, a 4 mm segmental bone defect was inflicted by 2 parallel osteotomies in the femur's midshaft using a gigli saw and a template. The operation wound was finally closed in two layers using sutures. The animals were allowed free movement for 8 weeks and were then sacrificed via an intracardiac injection of thiopentalsodium (Thiopental sandoz, Sandoz GmbH, Vienna, Austria) (120 mg/kg). Micro computertomograph (μCT) based detection of plate and/or screw dislocation at 4 or 8 weeks post surgery led to exclusion of the animal from μCT bone regeneration evaluation (8 out of 32 animals, 25% drop out).

Constitutive BMP2/7 co-expression in vivo

50μg constitutive co-expression plasmid pVAX1-BMP2/7- was co-delivered 3 days post surgery with 50μg of the internal luciferase control plasmid pCBR using sonoporation in the active gene transfer treatment group (total therapeutic DNA dose: 250μg; 0.5mg/kg). The luciferase control group consisted of animals sonoporated with 50μg of the internal luciferase control plasmid pCBR and 50μg of an empty pDNA backbone (pUK21, Plasmid Factory, Bielefeld, Germany) to normalize the DNA content according to the therapy group.

The efficacy of passive gene delivery to the defect was investigated using either injections of therapeutic plasmid co-delivered with the internal luciferase control plasmid (50μg pVAX1-BMP2/7- + 50μg pCBR) or of the internal luciferase control plasmid co-delivered with a non-expressing empty plasmid (50μg pCBR + 50μg pUK21) without ultrasound treatment. Furthermore, we investigated the endogenous regenerative potential and union rate in an empty control group, which did not receive any treatment. Sonoporation was carried out using the SP100 sonoporator and neutral, lipid-based microbubbles (MB101, Sonidel Ltd, Dublin, Ireland) at a final concentration of $8x10^8$/ml (75% v/v). 200μl of this plasmid-microbubble solution was injected under x-ray guidance and immediately after sonoporated into the femur defect site using the 4 Watt/cm^2 sonoporation protocol. This treatment was repeated for 5 days, resulting in a total therapeutic DNA dose of 250 μg/animal (~0.5mg/kg).

Plasmid DNA labelling & orthotopic detection

In order to enable therapeutic DNA detection at the defect site for biodistribution monitoring, we applied a novel metabolic DNA labelling method in *E.coli* based on the nucleoside (2'S)-2'-deoxy-2'-fluoro-5-ethynyluridine (F-*ara*-EdU) (Neef and Luedtke, 2011). pCBR plasmid DNA was labelled with F-*ara*-EdU using a thymidine-auxotrophic *E.coli* strain (Chi1776, DSMZ, Braunschweig, Germany) and supplementing 394 medium (Jerome *et al*., 2009)

containing 20mg/ml thymidine + 20mg/ml F-*ara*-EdU. Plasmids were isolated using the Endo-free Plasmid Maxi Kit (Qiagen, Hilden, Germany).

A separate cohort of rats (n=7) was allocated for imaging of *in situ* orthotopic luciferase expression and subsequent plasmid DNA detection 24h post last gene transfer. Detection was carried out on decalcified paraffin sections of the femora using an Alexa Fluor 680 labelled azide (Life Technologies, Palo Alto, CA, US) for the Cu^{+} catalyzed click reaction described in (Neef and Luedtke, 2011). AF680 signals, specific for F-*ara*-EdU labelled plasmid DNA were detected using an Odyssey near infrared scanner (LI-COR Biosciences, Lincoln, NE, US) and confocal laser scanning microscopy (CLSM). In CLSM, a separate 488nm channel was used in addition to the 680nm channel in order to use tissue autofluorescence to enable the generation of overlay images with specific AF680 signals and general tissue architecture. A decalcified femur control sample without F-*ara*-EdU labelled plasmid DNA served as a negative control.

Bioluminescence imaging

All nude mice that received the internal pCBR luciferase control plasmid were imaged 24h post last gene transfer in order to determine gene transfer efficacies. Imaging was carried out under short inhalation anaesthesia using a Xenogen IVIS100 Imaging system (Caliper Life Sciences GmbH, Mainz, Germany). Mice received 5mg D-luciferin potassium salt (Caliper Life Sciences GmbH, Mainz, Germany) in 300μl Ringer's solution (Mayerhofer Pharmazeutika GmbH, Linz, Austria) intraperitoneally before imaging. 20 minutes post D-luciferin administration, the mice were imaged for 2 minutes.

Sprague-Dawley rats were imaged 24h post last gene transfer in order to determine gene transfer efficacies. Imaging was carried out under short inhalation anaesthesia using a Xenogen IVIS100 Imaging system. Rats received 90mg D-luciferin potassium salt in 3ml Ringer's solution intraperitoneally before imaging. 30 minutes post D-luciferin administration, the rats were imaged for 2 minutes.

A separate group of rats was examined for gene transfer localization at the defect site 24h post last gene transfer using bioluminescence imaging *in vivo* after surgically opening the defect site (30min post luciferin administration) under general anaesthesia (see "femur-defect model" above). Additionally, femora were imaged *ex vivo* after the rats were sacrificed with in general anaesthesia (see above) by an overdose of thiopentalsodium (Thiopental, Sandoz GmbH, Vienna, Austria) (120 mg/kg) by intracardiac injection. Luciferase imaging was carried out after

explantation of the femur and adjacent muscles 45min post luciferin administration.

***In vivo* micro Computer Tomography (μCT) analysis**

In vivo μCT images of nude mouse hindlimbs were obtained using a VivaCT 75 (Scanco Medical AG, Brütisellen, Switzerland) 14 days and 28 days post last gene transfer under short inhalation anaesthesia. Bone volume (mm^3) and bone mineral density (mg hydroxyapatite per cm^3 (mg HA/cm^3)) for 2 and 28 days were calculated using Scanco software and a standard density calibration phantom.

In vivo μCT images of rat femora at 0, 4 and 8 weeks post surgery were exported into MATLAB (MATLAB version 7.12.0. The MathWorks Inc., 2012, Natick, MA, US) for processing. In order to facilitate analysis, the volumes corresponding to all 3 time points were rigidly registered onto each other using a three-step approach.

First, the supporting titanium plate was segmented using a manually determined grey-level threshold. When using such a simple segmentation procedure, image artefacts can lead to the erroneous segmentation of parts of the image as well as to the splitting of the titanium plate. To limit the influence of this onto subsequent steps of the analysis, only large elements of the segmentation were retained (> 3000 voxels).

In a second step, the major directions of the titanium plate were extracted from the processed binary segmentations using Principal Component Analysis (PCA, (Pearson, 1901)). Rotating the volumes according to these major axes serves as an initialization to the final matching step. For this, we employ the Iterative Closest Point (ICP, (Besl, 1992)) algorithm. While reliable in practice, it is well known to be susceptible to its initialization. Alignment using PCA assures the convergences of ICP to the correct matching between volumes.

The rotation computed using PCA and the deformation obtained after convergence of the ICP-process are combined into a rigid deformation matrix. This transformation was then applied to each volume in the sequence except the reference, ensuring the correct correspondences of each voxel between acquisition times.

All volumes were then represented as colour-coded overlays of the 3 time points. New bone at the defect site was segmented manually and quantified as bone volume/tissue (defect) volume.

Histology

Gastrocnemius muscles from nude mice were excised and fixed with 4% buffered paraformaldehyde (Sigma Aldrich GmbH, Vienna, Austria) in phosphate-buffered saline (PBS) for 24h, transferred in 50% ethanol and stored in 70% ethanol at 4°C. Samples were embedded in paraffin without decalcification, and several sections of the same sample were stained with haematoxylin and eosin (H&E) and von Kossa staining for mineralization according to standard histology protocols. Localization of the internal luciferase control expression was detected using the G7451 Goat Anti-Luciferase (Promega GmbH, Mannheim, Germany) primary antibody in a 1:50 dilution overnight and an appropriate secondary peroxidase conjugated antibody ImmPRESS Anti-Goat Ig Peroxidase (Vector Labs, Peterborough, UK) for 30min after blocking of endogenous peroxidase activity with 3% H_2O_2 in Tris-buffered saline. Nuclear counter-staining was carried out using Mayer's haematoxylin solution for 1min.

Statistical analysis

Results are represented as median±interquartile range unless otherwise stated. Statistical testing was carried out using the non-parametric Kruskal-Wallis test in conjunction with Dunn's multiple comparison test as post-test for luciferase expression, ectopic bone volume and bone mineral density data. Orthotopic sonoporation luciferase expression data did not pass normality testing (Kolmogorov-Smirnov test) and was therefore tested with the non-parametric Kruskal-Wallis test in conjunction with Dunn's multiple comparison test as post-test. Orthotopic passive luciferase expression data passed Kolmogorov-Smirnov normality testing and therefore was tested with a two-tailed t-test for significance. Gene transfer efficacy data (frequency of successful gene transfer) based on luciferase imaging and bone formation efficacy data (frequency of successful bone formation) were tested for improvement by sonoporation using a one-tailed Fisher's exact test. Bone volume per tissue volume (BV/TV) data from orthotopic models was confirmed to follow a Gaussian distribution and therefore tested with parametric ANOVA and Tukey's test for significance. $p<0.05$ was considered statistically significant (* $p<0.05$, ** $p<0.01$).

RESULTS

Ectopic BMP2/7 sonoporation

Gene transfer efficacies & luciferase gene expression

Evaluation of gene transfer efficacy 24 hours post last gene transfer via bioluminescence activity in nude mice confirmed successful gene transfer in 8 out of 13 animals (61% efficacy) for passive gene delivery, 6 out of 7 animals (85%) for 2 Watt/cm^2 sonoporation and 7/7 animals (100%) for 4 Watt/cm^2 sonoporation (Figure 1A). Bioluminescence imaging of the internal luciferase control demonstrated variable luciferase activity in all animals (Figure 1B) 24h post last treatment. No significant difference in bioluminescence levels was observed between passive gene transfer, 2 Watt/cm^2 or 4 Watt/cm^2 sonoporation. Sonoporation with 4 Watt/cm^2 caused considerable skin burns at the ultrasound exit sites in contrast to the 2 Watt/cm^2 protocol.

Ectopic bone formation using constitutive BMP2/7 co-expression in vivo

Passive gene delivery of the constitutive BMP2/7 co-expression plasmid pVAX1-BMP2/7- to successfully induced ectopic bone formation in 6 out of 13 animals (46%) (Figure 2A). Sonoporative gene delivery with either 2 or 4 Watt/cm^2 protocols successfully induced ectopic bone formation in 5 out of 7 (71%) or 7 out of 7 animals (100%) respectively (Figure 2A). 2 Watt/cm^2 sonoporation of pVAX1-BMP2/7- without the luciferase plasmid led to bone formation in 6 out of 7 animals (85%) (Figure 2A). Bone volumes were variable and did not exhibit significant differences (Figure 3G, H). Medians of bone volumes were 0.09 mm^3 at 14 days and 0.04 mm^3 at 28 days post treatment using the constitutive co-expression systems with passive gene transfer; 0.002 mm^3 (0.03 mm^3 without pCBR addition) at 14 days and 0.17 mm^3 (0.01 without CBR addition) at 28 days post treatment using the constitutive co-expression system with the 2 Watt/cm^2 sonoporation protocol and 0.02 mm^3 at 14 days and 0.01 mm^3 at 28 days post treatment using the constitutive co-expression system with the 4 Watt/cm^2 sonoporation protocol. Bone mineral densities did not show significant differences among treatment groups and different time points post treatment. Medians of bone mineral densities were 179.4 mg HA/cm^3 at 14 days and 238 mg HA/cm^3 at 28 days post treatment using the constitutive co-expression systems with passive gene transfer; 160 mg HA/cm^3 (201.8 mg HA/cm^3 without pCBR addition) at 14 days and 243.6 mg HA/cm^3 (230.4 mg HA/cm^3 without CBR addition) at 28 days post treatment using the constitutive co-expression system with the 2 Watt/cm^2 sonoporation protocol and

177.4 mg HA/cm^3 at 14 days and 220.7 mg HA/cm^3 at 28 days post treatment using the constitutive co-expression system with the 4 Watt/cm^2 sonoporation protocol. Ectopic bones displayed variable morphology and irregular shape in all observed treatment groups (representative images in Figure 3 A-F). Direct comparison of 14 day with 28 day *in vivo* μCT images of the same ossicles (Figure 3 A-F) showed moderate bone remodeling and resorption. Histological examination of ectopic bones at 4 weeks by HE staining revealed fully developed ossicles with a compact layer of bone surrounding a bone marrow cavity (Figure 4A) populated by a heterogenous cell population consisting of adipocytes, haematopoietic myeloid progenitor cells megakaryocytes and erythrocytes (Figure 4D). Immunohistochemical detection of the internal luciferase control showed diffuse staining in muscle fibers surrounding the ectopic bone structure and strong staining of bone lining and bone marrow cells (Figure 4B). Von Kossa staining for mineralization furthermore confirmed the observed structures in HE staining as mineralized bone tissue (Figure 4C).

Ectopic bone formation using inducible BMP2/7 co-expression in vivo

Sonoporation of the inducible single-vector BMP2/7 co-expression system pTetON-BMP2/7 using the 2 Watt/cm^2 sonoporation protocol successfully induced ectopic bone formation in 5 out of 6 animals (83%) only when induced with 2mg of doxycycline per 48h for 7 days as observed by *in vivo* μCT at 14 days and 28 days post treatment. No bone formation was observed without application of doxycycline (0 out of 6 animals) (Figure 2B). Furthermore, no bone formation was observed when using passive gene transfer and induction with 2mg of doxycycline per 48h for 7 days (Figure 2B). Ectopic bones did not show any significant differences in bone volumes (Figure 3G, H) or bone mineral densities compared to ectopic bones generated using the constitutive co-expression system pVAX1-BMP2/7- at 14 and 28 days post treatment. Medians of bone volumes were 0.1 mm^3 at 14 days and 0.01 mm^3 28 days post treatment using the inducible co-expression system with the 2 Watt/cm^2 sonoporation protocol. Medians of bone mineral densities were 149.7 mg HA/cm^3 at 14 days and 249.6 mg HA/cm^3 at 28 days post treatment.

Orthotopic BMP2/7 sonoporation

Orthotopic luciferase gene expression & gene transfer efficacies

Orthotopic bioluminescence imaging demonstrated strong luciferase expression limited to the defect site (Figure 5B, C, D) and no activity in adjacent muscle tissue (Figure 5C). No difference in localization and gene expression levels

was observed between sonoporation and passive gene transfer (Figure 1D). A significant reduction of bioluminescence was observed for both passive gene transfer and sonoporation when the luciferase plasmid was co-administered with pVAX1-BMP2/7- (Figure 1D), indicating potential competitive expression. Gene transfer efficacies estimated via bioluminescence imaging were 66% (6 out of 9 animals) for passive gene transfer and 85% (12 out of 14 animals) for the 4 Watt/cm^2 sonoporation group (Figure 1C).

Orthotopic F-ara-EdU labeled luciferase plasmid DNA distribution

Detection of luciferase plasmid DNA biodistribution 24h post last gene transfer at the defect site through near infrared scanning (Figure 6A) revealed extensive signals in bone tissue. In depth examination through CLSM demonstrated the confined presence of plasmid DNA within cells of the bone marrow (Figure 6B), at the defect site granulation tissue (Figure 6C), diffuse distribution of plasmid DNA within intact bone tissue (Figure 6D) and weak diffuse signals in surrounding muscle fibers (Figure 6E) with confined signals in satellite cells (Figure 6E, arrows). No differences in biodistribution were observed between passive gene transfer and sonoporation groups.

Orthotopic bone regeneration using constitutive BMP2/7 co-expression in vivo

In vivo μCT images of defects at 4 and 8 weeks post surgery showed 3 potential unions with substantial bone growth out of 6 animals of the sonoporation treatment group (Figure 7A), 1 potential union in the passive gene transfer treatment group (Figure 7B), 1 potential union in the luciferase control group (Figure 7C) and 1 potential union in the empty control group (Figure 7D) at 8 weeks post surgery. In depth examination of the μCT images at different angles and cut planes confirmed 2 unions out of 6 animals (33% union rate, Figure 8A) in the treatment group (Figure 7A, asterisks) and 1 union (16% union rate. Figure 8A) in the passive gene transfer treatment group (Figure 7B, asterisk) at 8 weeks post surgery. No unions were confirmed (Figure 8A) in the luciferase control and empty control groups 8 weeks post surgery (Figure 7C, D). Quantification of bone volume/tissue volume at the initial margins of the defect did not show any significant differences between treatment groups and controls at both 4 weeks (Figure 8B) and 8 weeks (Figure 8C) post surgery.

DISCUSSION

The aim of this study was to evaluate constitutive or regulated, doxycycline inducible, non-viral sonoporative BMP2/7 gene co-delivery *in vivo* for bone regeneration. It has been demonstrated that the repeated co-delivery of a highly bioactive BMP2/7 gene-combination effectively mediates bone formation *in vivo* and that gene expression can be precisely controlled. Direct comparison of sonoporation with passive gene delivery demonstrated an increased probability of gene expression and bone formation dependent on total ultrasound energy applied, whereas when successful gene transfer was accomplished, gene expression levels and bone volumes were not increased via sonoporation. In orthotopic models, a beneficial effect of sonoporation on gene transfer probabilities was indicated and to localized orthotopic gene expression was achieved. DNA tracking revealed that a large fraction of plasmid DNA binds to intact bone and is thus absorbed from the defect site. *In* vivo μCT data suggests enhanced orthotopic bone regeneration after active sonoporative gene transfer of BMP2/7 to the target site.

Ectopic BMP2/7 sonoporation

Ectopic gene transfer monitoring with luciferase showed that the rate of successful gene transfer can be increased compared to passive gene delivery when applying ultrasound of increasing power (Figure 1A). It was possible to reach gene transfer efficacies of 100% using the 4 Watt/cm^2 (600 Joule/cm^2) sonoporation protocol, however there were no significant differences in expression levels observed between passive gene transfer and sonoporation (Figure 1B). Therefore, we conclude that sonoporation increases gene transfer efficacy compared to passive gene delivery and that the efficacy depends on the applied ultrasound power. This is in line with findings demonstrated in (Li *et al*., 2009), showing that *in vitro* there is a delicate balance between ultrasound power, cell viability and sonoporation efficacy. We observed skin burning at the exit sites of ultrasound in the 4 Watt/cm^2 protocol in nude mice, which has not been reported in (Osawa *et al*., 2009), which used an outbred mice strain in which skin damage is less obvious. This phenomenon disappeared when ultrasound power was reduced from 600 Joule/cm^2 to 90 Joule/cm^2 using the 2 Watt/cm^2 protocol. Bone formation efficacies of the different gene transfer protocols (Figure 2) generally paralleled gene transfer efficacies observed by luciferase monitoring (Figure 1A) improving significantly with increasing ultrasound power.

BMP2/7 co-expression is considered highly effective as reported by several *in vitro* and *in vivo* studies (Kawai *et al*., 2006; Kawai *et al*., 2009) due to the formation of a highly bioactive BMP2/7 heterodimeric growth factor (Israel *et al*., 1996; Kawai *et al*., 2009), which is less prone to inhibition by endogenous inhibitors (W Zhu, 2006) and

induces endogenous BMP4 expression (Kawai *et al*., 2006). By applying this co-expression strategy, we were able to achieve 100% bone formation efficacy at lower DNA doses (1/5 of the dose used in (Osawa *et al*., 2009) with BMP2; 1.5x less of the dose used in (Sheyn *et al*., 2008) with BMP9), lower number of repetitive treatments (5x vs 7x in (Osawa *et al*., 2009)) or lower total applied ultrasound power (600 Joule/cm^2 in 24h vs. 1500 Joule/cm^2 in 24h in (Sheyn *et al*., 2008)) when compared to similar studies using only single BMP gene transfer (Osawa *et al*., 2009; 2010; Sheyn *et al*., 2008). Therefore, we conclude that the selected co-expression strategy is superior to single factor expression in the case of BMPs and that this allows higher therapeutic efficacy while using an actual low-efficacy non-viral gene transfer method. It might be feasible in the future to enable less invasive sonoporative gene transfer to compete with current electroporation approaches (G Pelled, 2005; Kawai *et al*., 2006; Sheyn *et al*., 2008), which are currently more effective than sonoporation (Sheyn *et al*., 2008) but rely on invasive insertion of electrodes in contrast to minimally invasive transcutaneous application of ultrasound.

This study employed an internal luciferase control for gene transfer monitoring, which did not exhibit a significant detrimental effect on bone formation efficacy (Figure 2A) in the ectopic model. Therefore, we conclude that there is no substantial detrimental effect of adding a separate internal control plasmid in this setup. The authors would like to note, however, that the luciferase levels obtained in this study were lower than in previously unpublished data for single luciferase sonoporation (Hofmann *et al*. 2013 in preparation), indicating competitive expression between internal control plasmids and therapeutic plasmids. *In vivo* quantitative μCT data showed no significant difference in bone volumes or bone mineral densities for passive gene transfer or sonoporation protocols in contrast to bone formation efficacy, which is in line with the findings on gene transfer efficacies described above. Bone volumes achieved by BMP2/7 gene delivery (passive or sonoporative) were comparable to ectopic bone volumes achieved with BMP9 sonoporation in (Sheyn *et al*., 2008). Average bone mineral densities were within the range of ectopic bone mineral densities expected in ectopic bone formation models (Usas *et al*., 2009; Wijdicks *et al*., 2009) but lower when compared to BMP9 sonoporative gene transfer (Sheyn *et al*., 2008). Average bone volumes, determined in this this study and in (Sheyn *et al*., 2008) in contrast to other BMP gene delivery work, however, are still limited, if compared to approaches which use biomaterials in conjunction with gene delivery or growth factor delivery (Bessa *et al*., 2010; Wegman *et al*., 2012). This is probably due to the template function of biomaterials, which provides a templating environment in contrast to the solution injection approach used in this study. Therefore, it might be of interest if ectopic bone volumes could be increased by using sonoporation in conjunction with

biomaterials, such as hydrogels. Such an approach for matrix-assisted sonoporation (MAS) has already been demonstrated *in vitro* by our group (Nomikou *et al*., 2013) and therefore shall be investigated in future studies.

The observed ectopic bone structures were irregular in shape with multiple centres of ossification per animal (Figure 3A-F) representing individual foci of gene delivery, expected to be formed due to the chosen multiple injection strategy adapted from (Osawa *et al*., 2009) based on the facto that Osawa *et al*. (Osawa *et al*., 2009) and our own unpublished data showed that it was impossible to generate ectopic bones by single sonoporation, which indicates that gene expression levels obtained are still relatively low and not sufficient for osteoinduction via a single treatment. It is thus of great importance to modify the approach to a single gene delivery protocol by using more effective therapeutic transgenes in combination with a biomaterial as mentioned above in order to improve and spatially control bone formation *in vivo*. Histological examination the ectopic centres of ossification (Figure 4A, C, D) showed functional ectopic bone tissue with calcified compact bone (Figure 4C) surrounding a bone marrow cavity (Figure 4D), which hosted haematopoietic bone marrow. This formation of a stem cell niche after BMP gene delivery has been reported before (Osawa *et al*., 2009; Sheyn *et al*., 2008) and demonstrates that simple gene delivery without biomaterials, stem cells or recombinant growth factors can induce the formation of complex tissues *in vivo*. Furthermore, immunohistochemical staining for luciferase (Figure 4B) proved that luciferase recipient cells are participating in ectopic bone formation and present in the bone marrow cavity, indicating that endogenous transgene receptive cells are contributing to ectopic bone and bone marrow formation. These findings demonstrate that direct *in vivo* co-delivery of bone morphogenetic protein-encoding plasmids can provide a viable alternative to stem cell or recombinant protein based therapies. Furthermore, the data presented herein clearly indicates that sonoporative gene delivery is superior in direct comparison with passive gene delivery with regards to gene transfer probability and that gene transfer efficacies are dependent on the total amount of ultrasound energy applied to the target site.

Inducible BMP2/7 co-expression in vivo

Doxycycline inducible BMP2/7 co-expression from a modified (Feichtinger *et al*. 2013, under review) bidirectional TetON system (Baron U, 1995) showed effective (83% efficacy) bone formation only when applied with ultrasound and only if gene expression from the system was activated by systemic application of doxycycline for 7 days (Figure 2B). This clearly showed tight co-expression control of 2 individual transgenes *in vivo* by systemic application of an

inductor. By narrowing *in vivo* BMP2/7 co-expression down to approximately 7 days, it was possible to demonstrate that even this short time window of *in vivo* BMP expression, recapitulating endogenous expression patterns (Yu *et al*., 2010), is sufficient for *in vivo* bone formation. This reduction of therapeutic gene dose and therapeutic gene expression time in comparison to the constitutive co-expression systems enabled us to clearly demonstrate the effect of sonoporation on bone formation efficacy (Figure 2B). Notably, potentially due to the reduced gene dose and/or expression time compared to the constitutive system, it was not possible to induce bone formation by passive gene transfer even in animals that received doxycycline treatment. Therefore, we conclude that sonoporation in general increases gene transfer efficacy and enables reduction of therapeutic gene dose and therapeutic gene expression time due to higher overall gene transfer efficacies & expression, which was not observed as dramatically with the constitutive co-expression systems, because overall gene expression levels were probably already saturated in contrast to the inducible system.

Orthotopic BMP2/7 sonoporation

Using X-ray guided repeated DNA injection to the defect site it was possible to achieve spatially controlled gene transfer to the target site *in vivo* without off-target expression in adjacent tissues (Figure 5A-D). Gene transfer efficacies were higher when using sonoporation as compared to passive gene transfer (Figure 1C), demonstrating the feasibility of using ultrasound for orthotopic gene delivery. Interestingly, in contrast to the ectopic findings, there was a significant decrease in luciferase activity when the luciferase plasmid was co-applied with the constitutive BMP2/7 co-expression plasmid in passive and sonoporative gene transfer (Figure 1D). This indicates that competitive expression might reduce overall gene expression efficacy if multiple independent expression entities are applied *in vivo*. Therefore we based gene transfer efficacy calculations only on the groups, which exclusively received the luciferase plasmid to rule out false negative signals observed due to competitive expression in animals that received both plasmids. Tracking of plasmid DNA biodistribution at the defect site (Figure 6) using a novel metabolic DNA labelling method based on the work of Neef *et al*. (Neef and Luedtke, 2011) showed a different picture than tracking of luciferase gene expression at the target site. It has been observed that the DNA spreads from the site of application to unintended tissues such as bone marrow, intact bone and surrounding muscles. Whereas expression at these sites could not be evaluated due to the limitations of luciferase imaging, it has been shown by other studies that the presence of plasmid DNA at off-target sites does not automatically trigger off-target transgene

expression (Coelho-Castelo *et al*., 2006) and this should therefore be carefully investigated in future studies before conclusions about off-target expression can be made. The most striking finding of plasmid DNA biodistribution monitoring was the extensive binding of DNA to intact bone indicating that the applied DNA gets absorbed by bone tissue. Binding of nucleic acids to ceramic hydroxyapatite has been well known already for some time (Kothari and Shankar, 1974; Mazin, 1977) and harnessed for DNA purification (Shan *et al*., 2012) and delivery (Choi and Murphy, 2010; Zhang *et al*., 2011). This study, however, is the first study to demonstrate this effect *in vivo* with biological hydroxyapatite and naked exogenous DNA in orthopaedic gene delivery. This absorption might be considered as another caveat in *in vivo* naked DNA transfer, additionally to nuclease digestion (Houk *et al*., 1999; Ribeiro *et al*., 2004) and should be considered in future studies as a parameter potentially responsible for low therapeutic efficacy of these approaches in bone regeneration at relatively high doses of DNA (Bonadio *et al*., 1999; Schwabe *et al*., 2012). *In vivo* quantitative and qualitative μCT data, although no significant difference could be found within this study design, indicate a potential beneficial effect of BMP2/7 gene delivery on regeneration. The 4mm femur segmental defect model used in this study had an overall non-union rate of 83% at 8 weeks post surgery. After in depth μCT evaluation of the empty control group, non-union rate of the model was determined to be 100% (0% union rate) and was therefore performing comparably to previous studies in rats by our group (Schmidhammer *et al*., 2006; Schutzenberger *et al*., 2012). It has been demonstrated that orthotopic BMP2/7 sonoporation leads to 2/6 confirmed unions (33% union rate) and passive gene delivery could achieve at least 1/6 unions (16% union rate) compared to 0/6 unions in both the negative luciferase control and empty defect control groups respectively when carefully evaluated by μCT, which has been shown to be the only reliable method in determining union rate (Schmidhammer *et al*., 2006). Therefore, and in conjunction with luciferase data, we conclude that sonoporative gene transfer enables orthotopic gene delivery and that orthotopic BMP2/7 sonoporation enhances bone regeneration at orthotopic sites. Thus, it might be possible to definitely prove therapeutic efficacy in future studies if the therapeutic effect is enhanced significantly either by additional recruitment of cells to a biomaterial *in situ* prior to gene delivery as demonstrated in (Kimelman-Bleich *et al*., 2011) or by combining our approach with the mentioned matrix-assisted sonoporation (MAS) technology (Nomikou *et al*., 2013). These potential modifications of the current protocol address different aspects, which potentially limited the therapeutic efficacy in this study, such as the initial lack of expression-capable cells at the defect site and DNA absorption from the target site by the surrounding intact bone tissue, given that an additional biomaterial could recruit endogenous cells and retain the therapeutic DNA at

the site of action. Furthermore, our data indicated that application of an internal luciferase control reduces gene expression at the defect site due to competitive expression. Therefore, therapeutic efficacy could be enhanced in future studies by applying only the therapeutic co-expression plasmid without the internal luciferase control.

Non-specific influence of ultrasound on bone regeneration in vivo

Ultrasound stimulation is a well-known physical method to enhance osteogenic differentiation and bone regeneration *in vivo*. Specifically low-intensity ultrasound stimulation (LIPUS) has successfully been applied for this purpose *in vitro* (Ikeda *et al*., 2006), *in vivo* at ectopic sites (Watanuki *et al*., 2009) and for clinical treatment of non-union fractures (Griffin *et al*., 2008; Romano *et al*., 2009). Furthermore, it has been documented successfully that ultrasound-stimulation *in vivo* increases the volume of ectopic bone formation with recombinant human BMPs *in vivo* (Wijdicks *et al*., 2009), thus enabling a reduction in dose using LIPUS. Therefore, it is important to take into account potential non-specific effects of ultrasound stimulation on bone for the study described herein. Although non-specific effects of ultrasound on bone formation unrelated to gene transfer cannot be ruled out, it is unlikely that substantial effects of ultrasound occurred in this study. The ultrasound trigger used for gene delivery is of a different frequency (1MHz vs. 1,5Mhz for LIPUS) and uses substantially higher power intensities (90-600 Joule/cm^2/day compared to approximately 7 Joule/cm^2/day in LIPUS) and is considered a high-intensity ultrasound stimulus which can lead to tissue heating and damage not occurring in LIPUS treatment (Ikeda *et al*., 2006). LIPUS itself has however been shown to increase the therapeutic efficacy of non-virally delivered BMP expression plasmids (Watanuki *et al*., 2009) *in vivo* and could therefore be additionally employed in future studies to further increase therapeutic efficacy of gene therapeutic approaches. The luciferase control groups employed in this study did not show increased bone volumes compared to empty controls, therefore it is unlikely that the employed ultrasound had a significant impact on bone regeneration. While it is important to discuss implications of ultrasound stimulation on tissue regeneration, we did observed such effects in this study.

Acknowledgements

This work was funded by the EUROSTARS project E!5650 UGen. The authors want to acknowledge Alexandra Meinl for histology, Sabine Pfeifer for her professional help with the animal models, Martin Mayer for his help with

the *in vivo* μCT scans, Peadar O'Corragain from Sonidel Ltd. for his assistance and advice and Sushmita Saha for assitance in writing the manuscript.

Author Disclosure Statement

G. A. Feichtinger and H. Redl are academic collaborators/sub-contractors of the ultrasound gene transfer equipment manufacturer Sonidel Ltd. within the EUROSTARS project E!5650 UGen. N. Nomikou is employed by Sonidel Ltd. for microbubble reagent development.

References

AXELRAD TW, KAKAR S, EINHORN TA. (2007). New technologies for the enhancement of skeletal repair. Injury 38 Suppl 1, S49-62.

BARON U FS, GOSSEN M, BUJARD H. (1995). Co-regulation of two gene activities by tetracycline via a bidirectional promoter. Nucleic Acids Research Sep 11; 23, 3605-3606.

BENGLIS D, WANG MY, LEVI AD. (2008). A comprehensive review of the safety profile of bone morphogenetic protein in spine surgery. Neurosurgery 62, ONS423-31; discussion ONS431.

BESL PJ. (1992). A method for registration of 3-D shapes. IEEE Trans on Pattern Analysis and Machine Intelligence 14, 239-256.

BESSA PC, BALMAYOR ER, HARTINGER J, ZANONI G*, et al*. (2010). Silk fibroin microparticles as carriers for delivery of human recombinant bone morphogenetic protein-2: in vitro and in vivo bioactivity. Tissue Eng Part C Methods 16, 937-45.

BLEIZIFFER O, ERIKSSON E, YAO F, HORCH F*, et al*. (2007). Gene transfer strategies in tissue engineering. J Cell Mol Med 11, 206-223.

BONADIO J, SMILEY E, PATIL P, GOLDSTEIN S. (1999). Localized, direct plasmid gene delivery in vivo: prolonged therapy results in reproducible tissue regeneration. Nat Med. Jul;5, 753-759.

BROOKS SA. (2006). Protein glycosylation in diverse cell systems: implications for modification and analysis of recombinant proteins. Expert Rev Proteomics 3, 345-59.

BRUDER SP, JAISWAL N, RICALTON NS, MOSCA JD*, et al*. (1998). Mesenchymal stem cells in osteobiology and applied bone regeneration. Clin Orthop Relat Res, S247-56.

CEMAZAR M, GOLZIO M, SERSA G, ROLS MP*, et al*. (2006). Electrically-assisted nucleic acids delivery to tissues in vivo: where do we stand? Curr Pharm Des 12, 3817-25.

CHOI S, MURPHY WL. (2010). Sustained plasmid DNA release from dissolving mineral coatings. Acta Biomater 6, 3426-35.

COELHO-CASTELO AA, TROMBONE AP, ROSADA RS, SANTOS RR, JR*., et al*. (2006). Tissue distribution of a plasmid DNA encoding Hsp65 gene is dependent on the dose administered through intramuscular delivery. Genet Vaccines Ther 4, 1.

G PELLED AL, Y ZILBERMAN, E ZEIRA, H YOTVAT, E GALUN, J LI, GA HELM, D GAZIT. (2005). Bone Regeneration Induced by Combining In Vivo Electroporation of an Osteogenic Gene and Human Mesenchymal Stem Cells. Molecular Therapy 11, S297-S297.

GAMRADT SC LJ. (2004). Genetic modification of stem cells to enhance bone repair. Ann Biomed ENg 32, 136-147.

GRIFFIN XL, COSTELLO I, COSTA ML. (2008). The role of low intensity pulsed ultrasound therapy in the management of acute fractures: a systematic review. J Trauma 65, 1446-52.

HOUK BE, HOCHHAUS G, HUGHES JA. (1999). Kinetic modeling of plasmid DNA degradation in rat plasma. AAPS PharmSci 1, E9.

HWANG CJ, VACCARO AR, LAWRENCE JP, HONG J*, et al*. (2009). Immunogenicity of bone morphogenetic proteins. J Neurosurg Spine 10, 443-51.

IKEDA K, TAKAYAMA T, SUZUKI N, SHIMADA K*, et al*. (2006). Effects of low-intensity pulsed ultrasound on the differentiation of C2C12 cells. Life Sci 79, 1936-43.

ISRAEL DI, NOVE J, KERNS KM, KAUFMAN RJ*, et al*. (1996). Heterodimeric bone morphogenetic proteins show enhanced activity in vitro and in vivo. Growth Factors 13, 291-300.

JEROME V, HEIDER A, SCHALLON A, FREITAG R. (2009). Exhaustive in vivo labelling of plasmid DNA with BrdU for intracellular detection in non-viral transfection of mammalian cells. Biotechnol J 4, 1479-87.

JONES CB MK. (2005). Nonunion treatment: iliac crest bone graft techniques. J Orthop Trauma. 19, 11-13.

KANAKARIS NK, GIANNOUDIS PV. (2008). Clinical applications of bone morphogenetic proteins: current evidence. J Surg Orthop Adv 17, 133-46.

KAWAI M, BESSHO K, MARUYAMA H, MIYAZAKI J*, et al*. (2006). Simultaneous gene transfer of bone morphogenetic protein (BMP) -2 and BMP-7 by in vivo electroporation induces rapid bone formation and BMP-4 expression. BMC Musculoskelet Disord. Aug 3;7:62, 1471-2474.

KAWAI M, MARUYAMA H, BESSHO K, YAMAMOTO H*, et al*. (2009). Simple strategy for bone regeneration with a BMP-2/7 gene expression cassette vector. Biochem Biophys Res Commun 390, 1012-7.

KIMELMAN-BLEICH N, PELLED G, ZILBERMAN Y, KALLAI I*, et al*. (2011). Targeted gene-and-host progenitor cell therapy for nonunion bone fracture repair. Mol Ther 19, 53-9.

KOTHARI RM, SHANKAR V. (1974). RNA fractionation on hydroxyapatite columns. J Chromatogr 98, 449-75.

LI YS, DAVIDSON E, REID CN, MCHALE AP. (2009). Optimising ultrasound-mediated gene transfer (sonoporation) in vitro and prolonged expression of a transgene in vivo: potential applications for gene therapy of cancer. Cancer Lett 273, 62-9.

LUO J, SUN MH, KANG Q, PENG Y*, et al*. (2005). Gene therapy for bone regeneration. Curr Gene Ther 5, 167-79.

MAZIN AL. (1977). [Hydroxyapatite thin-layer chromatography of nucleic acid]. Mol Biol (Mosk) 11, 477-98.

MK SEN TM. (2007). Autologous iliac crest bone graft: Should it still be the gold standard for treating nonunions? Injury 38S1, 75-80.

NEEF AB, LUEDTKE NW. (2011). Dynamic metabolic labeling of DNA in vivo with arabinosyl nucleosides. Proc Natl Acad Sci U S A 108, 20404-9.

NOMIKOU N, FEICHTINGER GA, REDL H, MCHALE AP. (2013). Ultrasound-mediated gene transfer (sonoporation) in fibrin-based matrices: potential for use in tissue regeneration. J Tissue Eng Regen Med.

OSAWA K, OKUBO Y, NAKAO K, KOYAMA N*, et al*. (2009). Osteoinduction by microbubble-enhanced transcutaneous sonoporation of human bone morphogenetic protein-2. J Gene Med 11, 633-41.

OSAWA K, OKUBO Y, NAKAO K, KOYAMA N*, et al*. (2010). Osteoinduction by repeat plasmid injection of human bone morphogenetic protein-2. J Gene Med 12, 937-44.

PEARSON K. (1901). On Lines and Planes of Closest Fit to Systems of Points in Space. Philosophical Magazine 2, 559-572.

RIBEIRO SC, MONTEIRO GA, PRAZERES DM. (2004). The role of polyadenylation signal secondary structures on the resistance of plasmid vectors to nucleases. J Gene Med 6, 565-73.

ROMANO CL, ROMANO D, LOGOLUSO N. (2009). Low-intensity pulsed ultrasound for the treatment of bone delayed union or nonunion: a review. Ultrasound Med Biol 35, 529-36.

S MEHIER-HUMBERT RG. (2005). Physical methods for gene transfer: Improving the kinetics of gene delivery into cells. Advanced Drug Delivery Reviews 57, 733-753.

SCHMIDHAMMER R, ZANDIEH S, MITTERMAYR R, PELINKA LE*, et al*. (2006). Assessment of bone union/nonunion in an experimental model using microcomputed technology. J Trauma 61, 199-205.

SCHMIDMAIER G, SCHWABE P, STROBEL C, WILDEMANN B. (2008). Carrier systems and application of growth factors in orthopaedics. Injury 39 Suppl 2, S37-43.

SCHUTZENBERGER S, SCHULTZ A, HAUSNER T, HOPF R, *et al*. (2012). The optimal carrier for BMP-2: a comparison of collagen versus fibrin matrix. Arch Orthop Trauma Surg 132, 1363-70.

SCHWABE P, GREINER S, GANZERT R, EBERHART J, *et al*. (2012). Effect of a Novel Nonviral Gene Delivery of BMP-2 on Bone Healing. ScientificWorldJournal 2012, 560142.

SHAN Z, LI X, GAO Y, WANG X, *et al*. (2012). Application of magnetic hydroxyapatite nanoparticles for solid phase extraction of plasmid DNA. Anal Biochem 425, 125-7.

SHEYN D, KIMELMAN-BLEICH N, PELLED G, ZILBERMAN Y, *et al*. (2008). Ultrasound-based nonviral gene delivery induces bone formation in vivo. Gene Ther 15, 257-66.

STANNARD J, SCHMIDT A, KREGOR P. (2007). *Surgical treatment of orthopaedic trauma*. Thieme Medical Publishers.

USAS A, HO AM, COOPER GM, OLSHANSKI A, *et al*. (2009). Bone regeneration mediated by BMP4-expressing muscle-derived stem cells is affected by delivery system. Tissue Eng Part A 15, 285-93.

VAIBHAV B, NILESH P, VIKRAM S, ANSHUL C. (2007). Bone morphogenic protein and its application in trauma cases: a current concept update. Injury 38, 1227-35.

VERBEEK R. (2012). Generation of mesenchymal stem cells as a medicinal product in organ transplantation. Curr Opin Organ Transplant.

W ZHU JK, C CHENG, BA RAWLINS, O BOACHIE-ADJEI, RG CRYSTAL, C HIDAKA. (2006). Noggin regulation of bone morphogenetic protein (BMP) 2/7 heterodimer activity in vitro. Bone 39, 61-71.

WATANUKI M, KISHIMOTO KN, KOTAJIMA S, IWABUCHI S, *et al*. (2009). Effect of low-intensity pulsed ultrasound on scaffold-free ectopic bone formation in skeletal muscle. Ups J Med Sci 114, 242-8.

WEGMAN F, GEUZE RE, VAN DER HELM YJ, CUMHUR ONER F, *et al*. (2012). Gene delivery of bone morphogenetic protein-2 plasmid DNA promotes bone formation in a large animal model. J Tissue Eng Regen Med.

WIJDICKS CA, VIRDI AS, SENA K, SUMNER DR, *et al*. (2009). Ultrasound enhances recombinant human BMP-2 induced ectopic bone formation in a rat model. Ultrasound Med Biol 35, 1629-37.

YU YY, LIEU S, LU C, MICLAU T, *et al*. (2010). Immunolocalization of BMPs, BMP antagonists, receptors, and effectors during fracture repair. Bone 46, 841-51.

ZHANG W, TSURUSHIMA H, OYANE A, YAZAKI Y, *et al*. (2011). BMP-2 gene-fibronectin-apatite composite layer enhances bone formation. J Biomed Sci 18, 62.

ZHAO M, ZHAO Z, KOH JT, JIN T, *et al*. (2005). Combinatorial gene therapy for bone regeneration: cooperative interactions between adenovirus vectors expressing bone morphogenetic proteins 2, 4, and 7. J Cell Biochem. May 1; 95, 1-16.

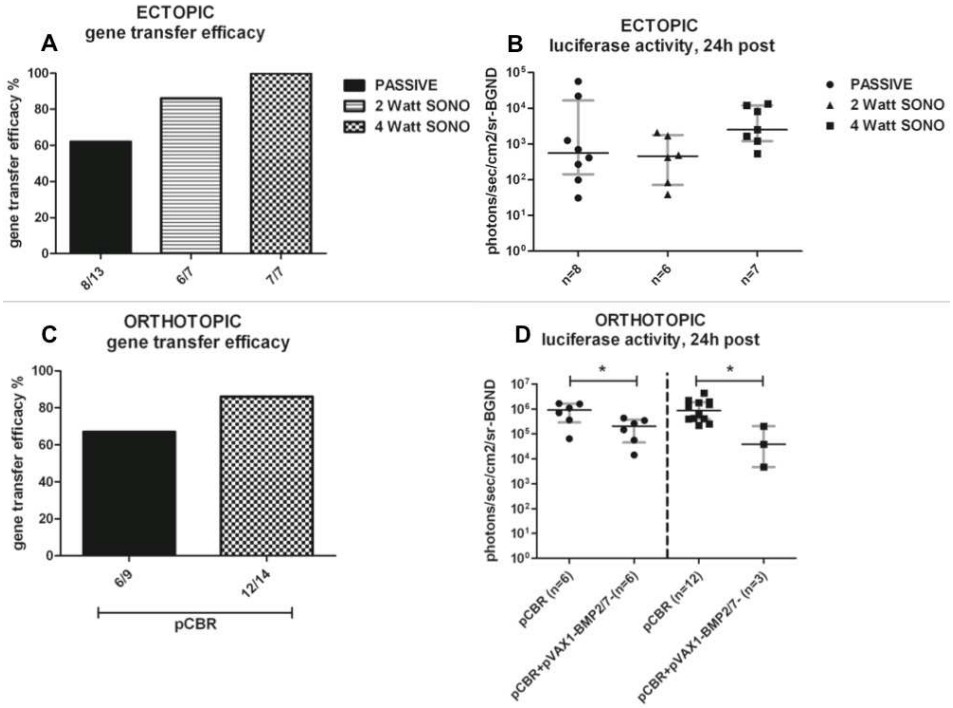

Figure 1: Influence of sonoporation on orthotopic and ectopic gene transfer efficacies.

Ectopic (A) and orthotopic (C) gene transfer efficacies based on luciferase activity. Ectopic luciferase activity (BMP2/7 and luciferase co-delivery) (B) and orthotopic luciferase activity (only luciferase: „pCBR“ vs. luciferase and BMP2/7 co-delivery: „pCBR+pVAX1-BMP2/7-„) (D) 24 hours post last gene transfer for passive and sonoporative gene delivery. Median ± interquartile range.

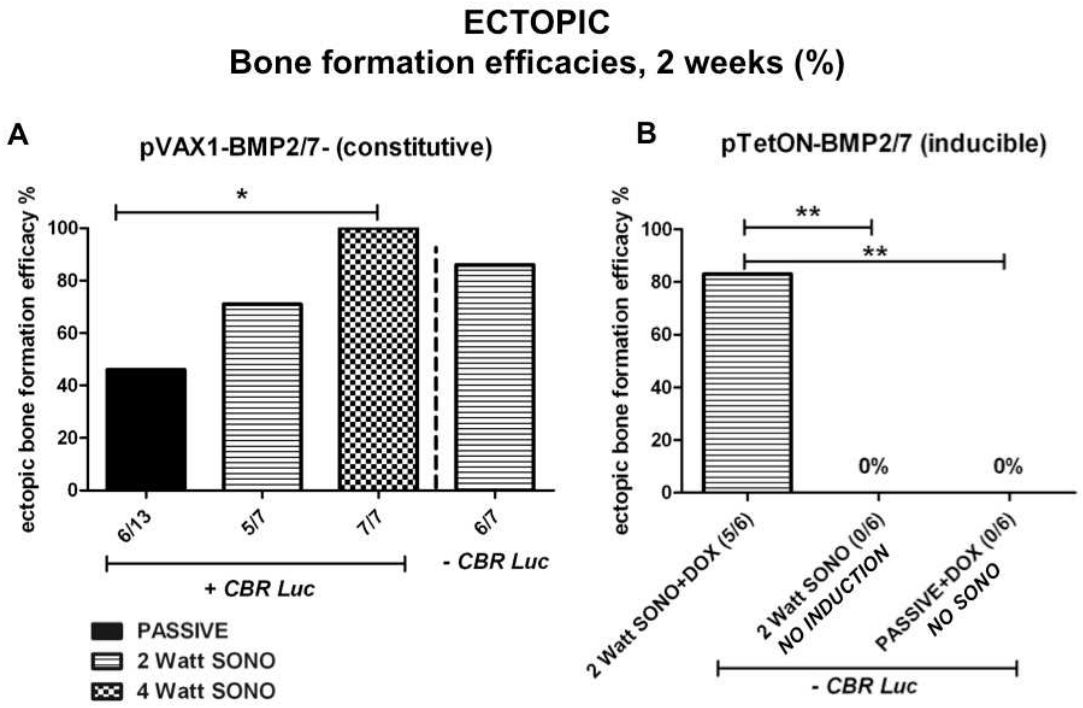

Figure 2: Enhancement of ectopic bone formation efficacy by sonoporation and effect of doxycycline on controlled bone formation (inducible BMP2/7 co-expression system).

Ectopic bone formation efficacies (frequency of successful bone formation after gene delivery) for constitutive pVAX1-BMP2/7- based co-expression experiments (A) with and without luciferase plasmid addition (+CBR Luc/-CBR Luc). Ectopic bone formation efficacies (frequency of successful bone formation after gene delivery) for inducible pTetON-BMP2/7 based co-expression experiments (B) without luciferase plasmid addition and with or without doxycycline (DOX) application. Results represented for passive gene transfer and 2 Watt/cm^2 and 4 Watt/cm^2 sonoporation protocols.

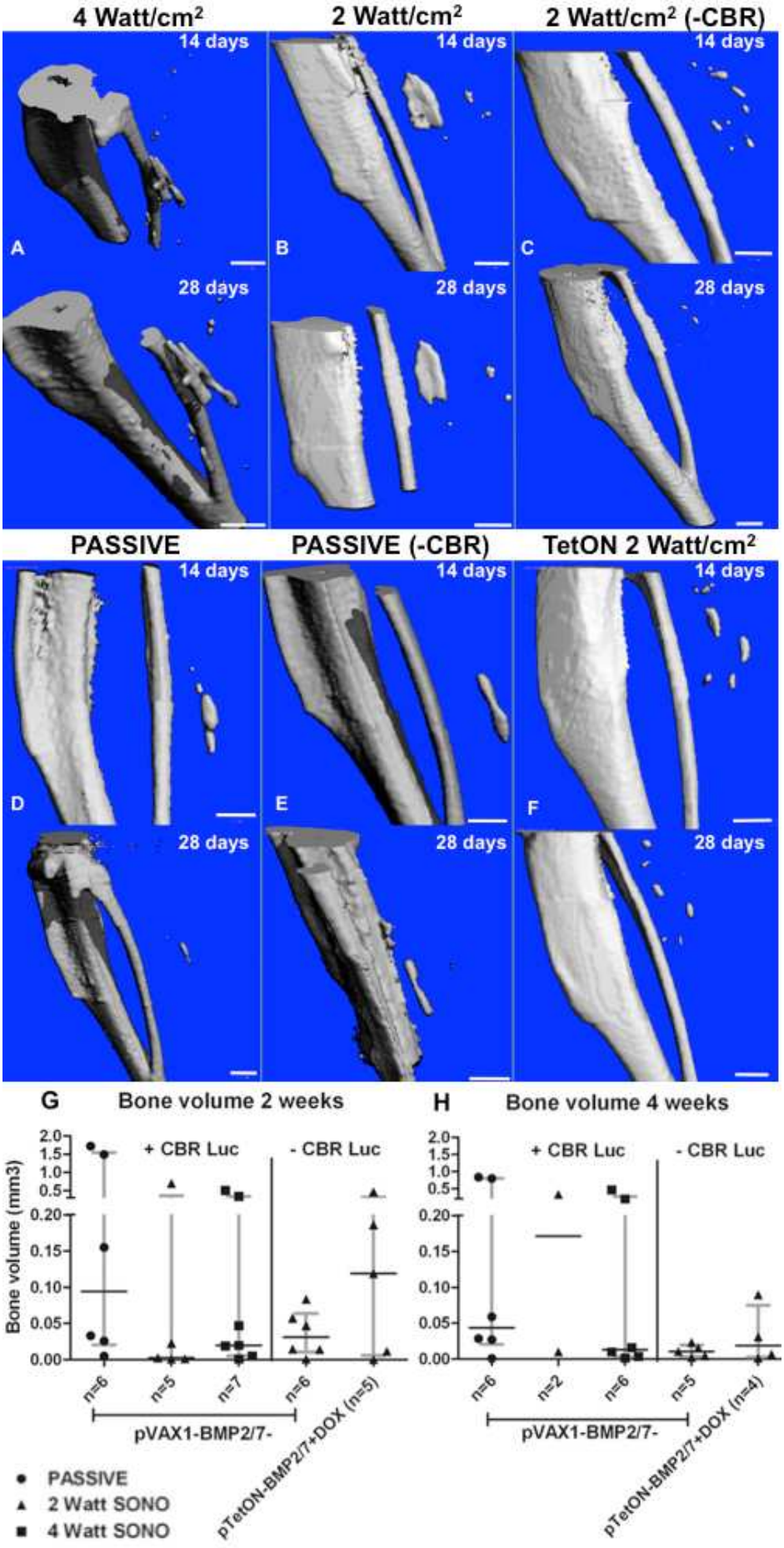
4 Watt/cm2
2 Watt/cm2
2 Watt/cm2 (-CBR)
14 days
28 days
A
B
C
PASSIVE
PASSIVE (-CBR)
TetON 2 Watt/cm2
D
E
F
G
Bone volume 2 weeks
H
Bone volume 4 weeks
+ CBR Luc
- CBR Luc
Bone volume (mm3)
2.0
1.5
1.0
0.5
0.20
0.15
0.10
0.05
0.00
n=6
n=5
n=7
n=6
n=6
n=2
n=6
n=5
n=4
pVAX1-BMP2/7-
pTetON-BMP2/7+DOX (n=5)
pTetON-BMP2/7+DOX (n=4)
PASSIVE
2 Watt SONO
4 Watt SONO

Figure 3: BMP2/7 co-expression induces ectopic bone formation *in vivo*.

Representative images of ectopic bones at 14 days and 28 days post treatment for 4 Watt/cm2 constitutive BMP2/7 co-expression system sonoporation ("4 Watt/cm^2") (A), 2 Watt/cm2 constitutive BMP2/7 co-expression system sonoporation ("2 Watt/cm^2") (B), 2 Watt/cm2 constitutive BMP2/7 co-expression system sonoporation without luciferase internal control ("2 Watt/cm^2 (-CBR)") (C), passive gene transfer of the constitutive BMP2/7 co-expression system ("PASSIVE") (D), passive gene transfer of the constitutive BMP2/7 co-expression system without luciferase ("PASSIVE (-CBR)") (E) and inducible BMP2/7 co-expression system without luciferase with 2 Watt/cm2 sonoporation protocol ("TetON 2 Watt/cm^2") (F). Scale bars represent 1mm. Quantitative *in vivo* μCT data for ectopic bones 2 weeks (G) and 8 weeks (H) post treatment. Median ± interquartile range.

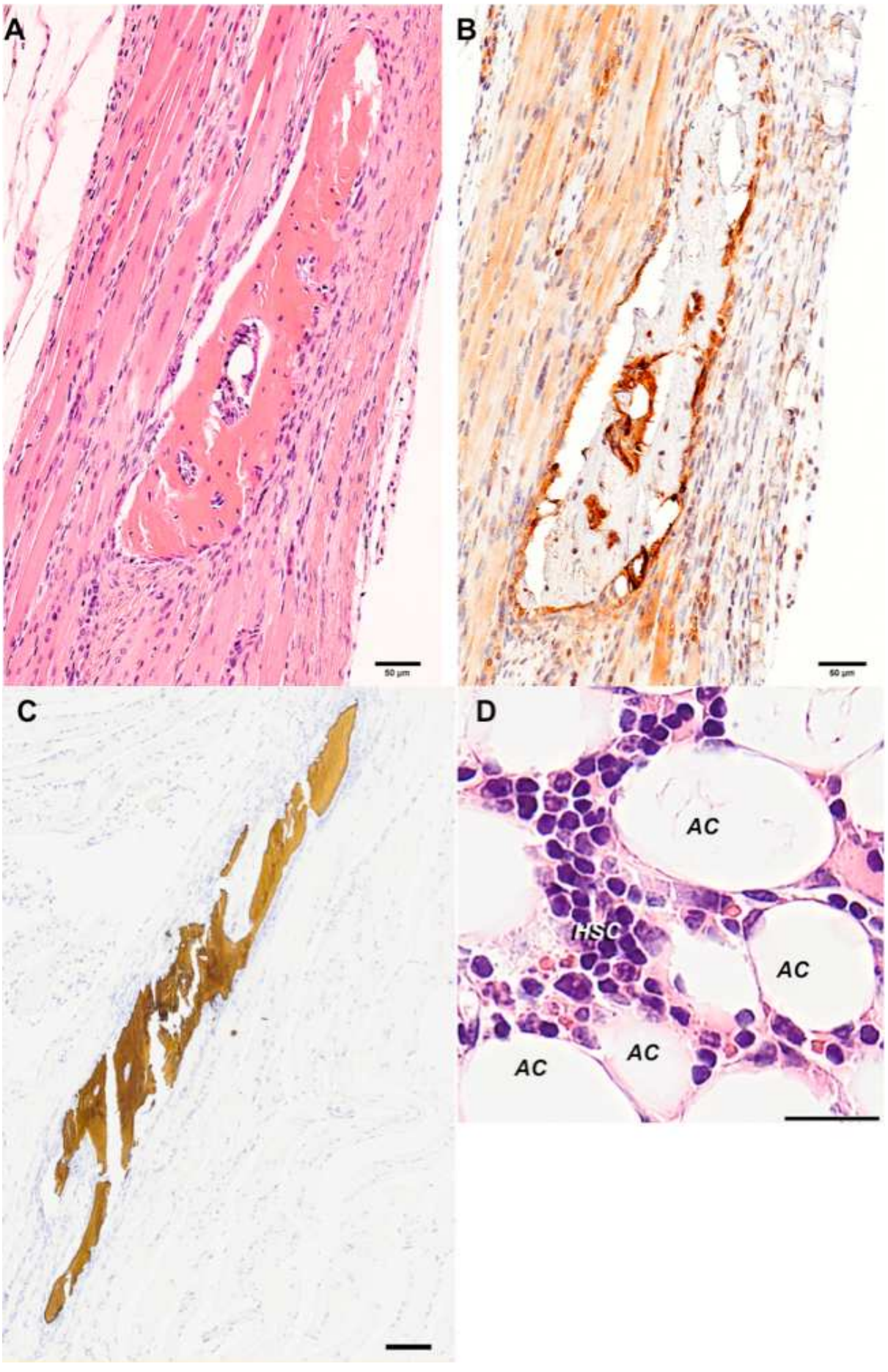
A
50 µm
B
50 µm
C
D
AC
HSC
AC
AC
AC

Figure 4: Formation of ectopic bone and a stem cell niche by BMP2/7 co-expression *in vivo*.

Histologies of ectopic bone (representative image of 4 Watt/cm2 sonoporation). Haematoxylin/Eosin staining (A), Immunohistochemical detection of luciferase (B), von Kossa staining for mineralization (C) and close-up of bone marrow of ectopic bones stained with haematoxylin/eosin (D) showing haematopoietic bone marrow with haematopoietic stem cells (HSC) and adipocytes (AC). Scale bars represent 50μm, in A, B and C and 20 μm in D.

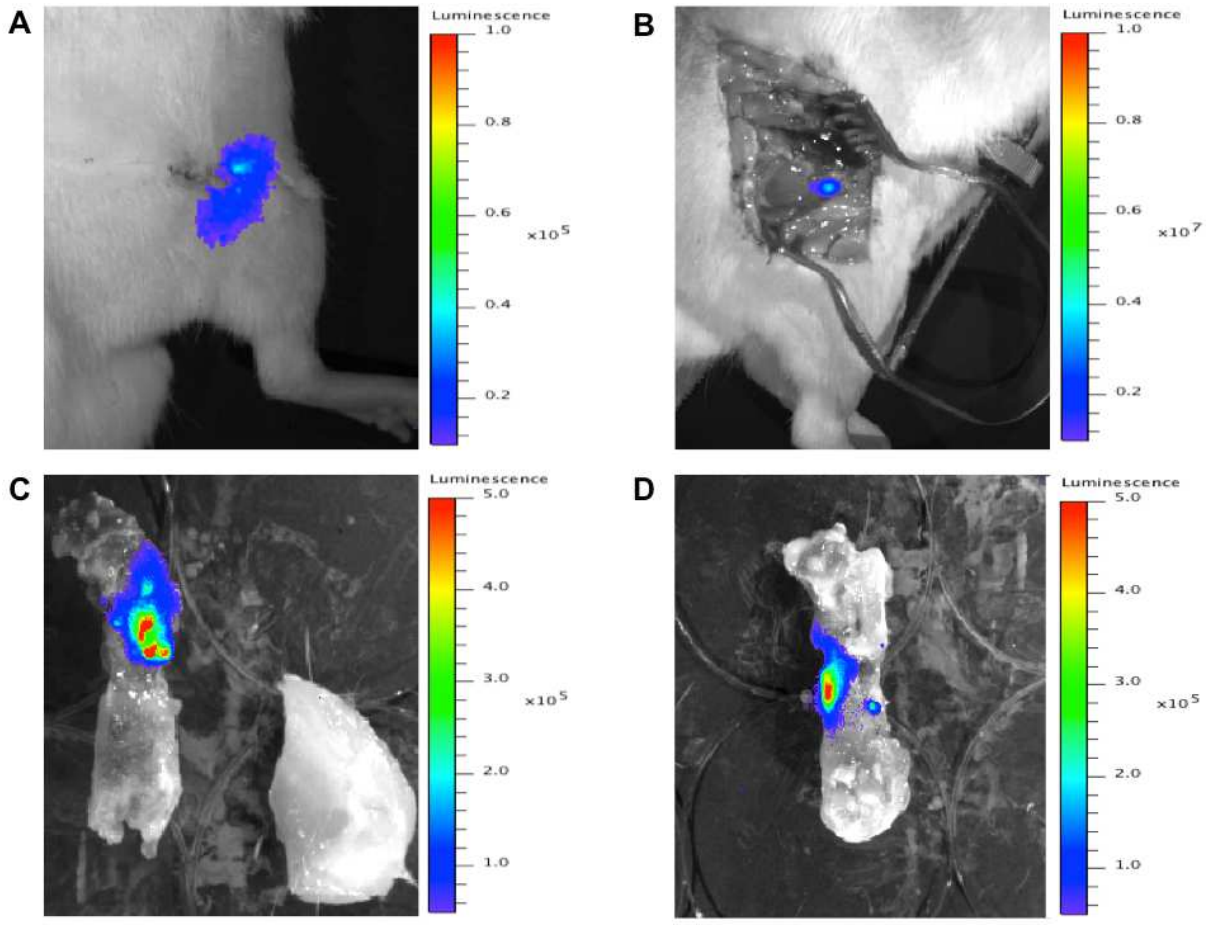

Figure 5: Spatially controlled orthotopic gene delivery *in vivo*.

Luciferase expression after orthotopic gene delivery. Bioluminescence activity in rat femurs depicted as false colour images of average photons/sec/cm^2/steradian (A: *in vivo*; B: *in situ*; C: *ex vivo*, femur & adjacent muscle; D: *ex vivo*).

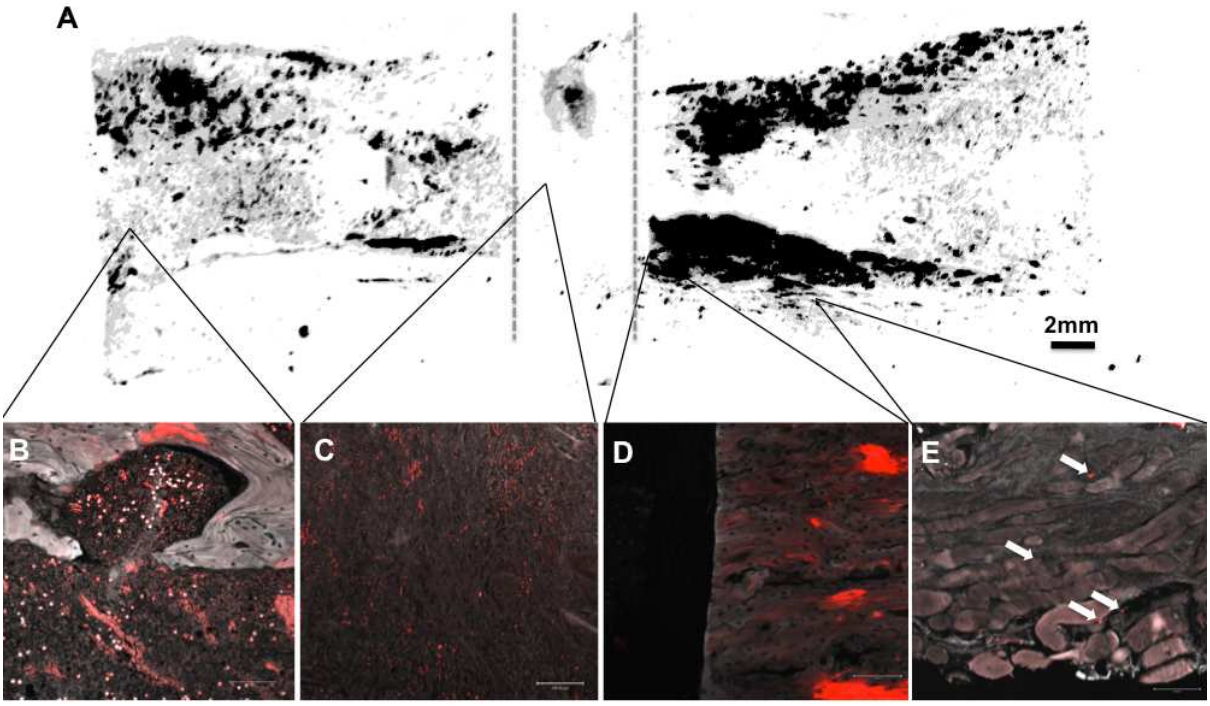

Figure 6: Plasmid DNA biodistribution and binding to intact bone in the defect area.

Orthotopic luciferase plasmid tracking using (2'S)-2'-deoxy-2'-fluoro-5-ethynyluridine (F-*ara*-EdU) metabolically labelled pCBR luciferase plasmid DNA detected with Alexa Fluor 680 azide 24 hours post last gene transfer. Odyssey near infrared scan of F-*ara*-EdU signals in a representative femur sample (A), scale bar represents 2mm. In-depth examination of selected areas using confocal laser scanning microscopy: femoral bone marrow cavity (B), defect granulation tissue (C), intact bone tissue of remaining femur stump (D) and surrounding muscle tissues (E). Scale bars represent 100μm.

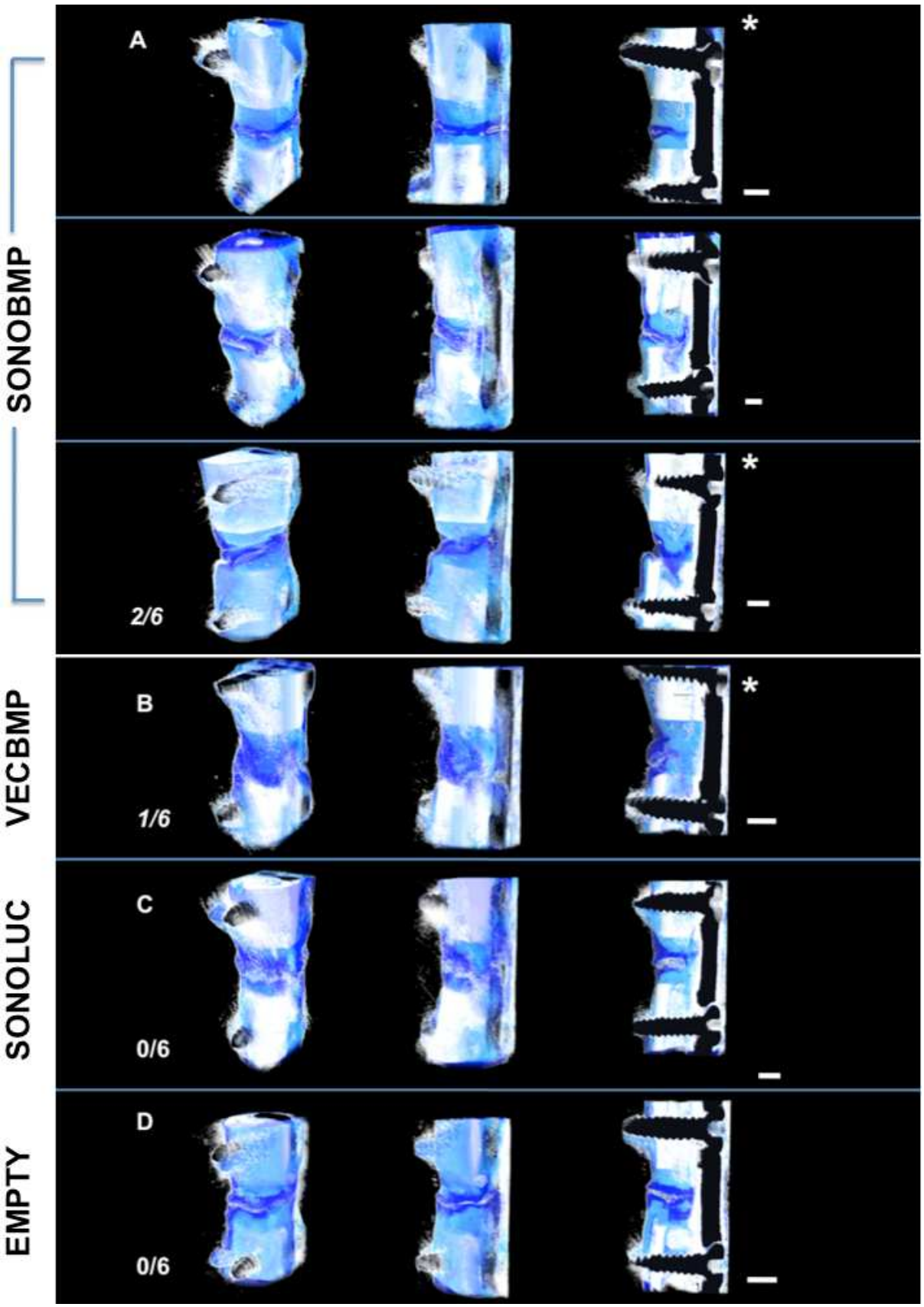
SONOBMP
VECBMP
SONOLUC
EMPTY
A
2/6
B
1/6
C
0/6
D
0/6
*
*
*

Figure 7: Bone regeneration in femur fractures by orthotopic BMP2/7 sonoporation.

Registered *in vivo* μCT images of potential unions each from different viewing angles and sagittal cut plane : 0 weeks (white), 4 weeks (light blue) and 8 weeks post fracture (dark blue) of potential unions in the sonoporation therapy group ("SONOBMP") (A), passive gene transfer therapy group ("VECBMP") (B), luciferase sonoporation control group ("SONOLUC") (C) and empty control group ("EMPTY") (D). Unions confirmed by in depth examination are marked with an asterisk. Scale bars represent 2mm.

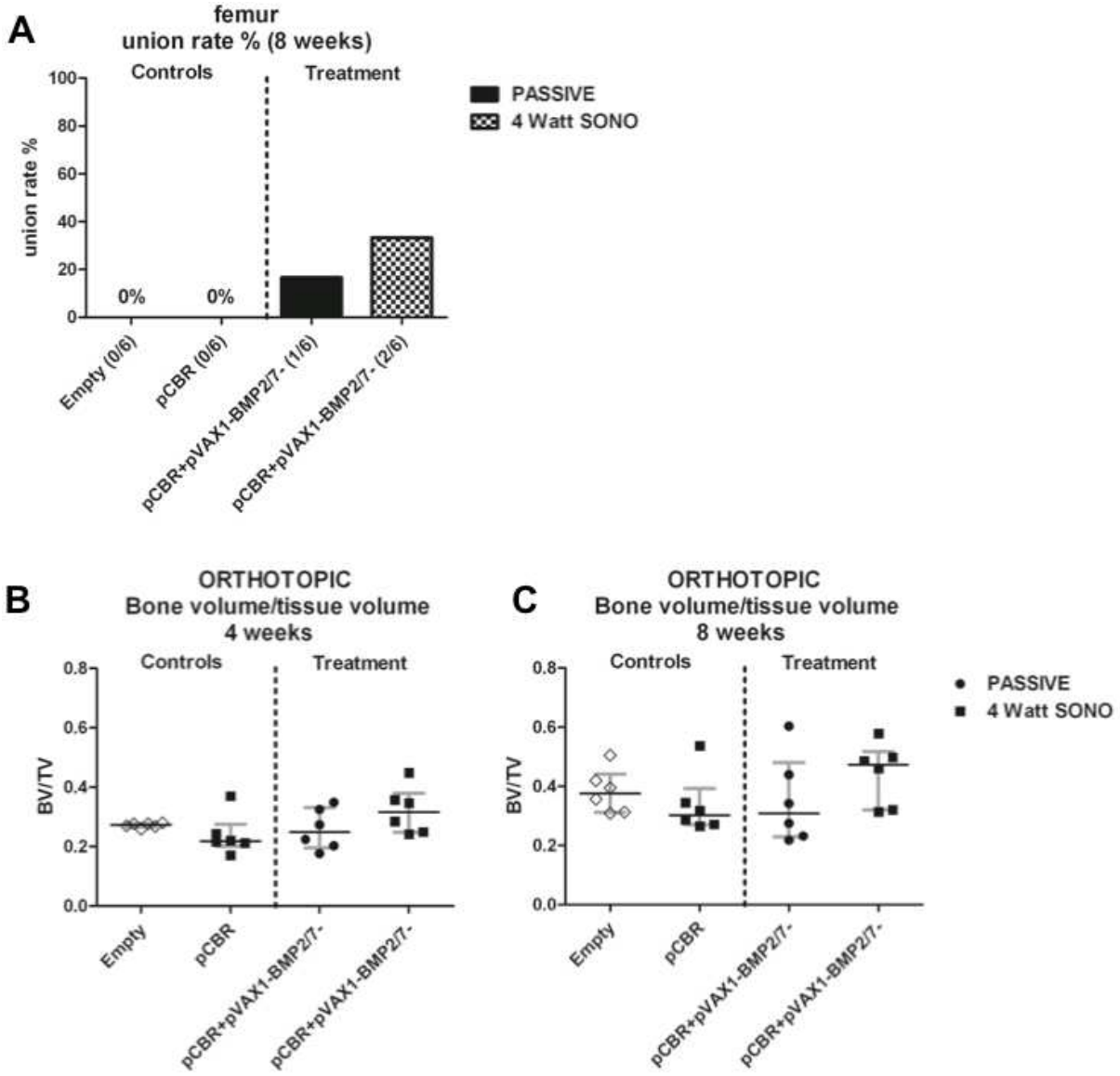

Figure 8: Effect of orthotopic BMP2/7 sonoporation on union rate.

Observed union rates based on in-depth μCT examination (A). Orthotopic bone volumes per defect tissue volumes based on quantitative *in vivo* μCT evaluation 4 weeks (B) and 8 weeks (C) post fracture. Empty control group („Empty“), luciferase control group („pCBR“) and treatment groups („pCBR+pVAX1-BMP2/7-“). Data depicted for passive gene transfer („PASSIVE“) and 4 Watt/cm2 sonoporation („4 Watt SONO“). n=6, Median±interquartile range.

A

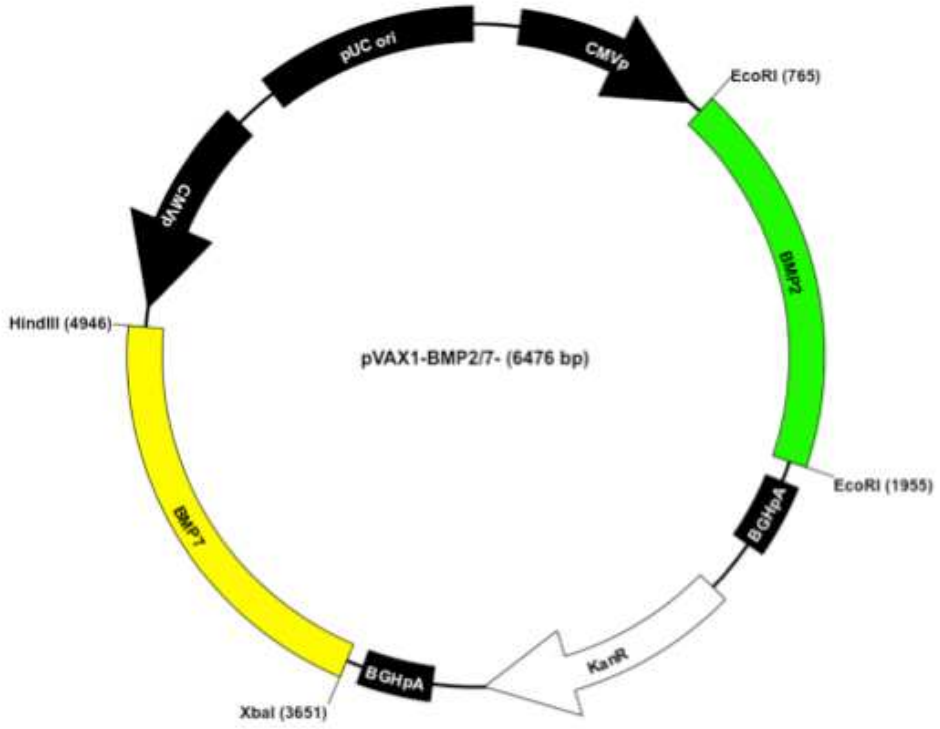
pUC ori
CMVp
EcoRI (765)
BMP2
EcoRI (1955)
BGHpA
KanR
BGHpA
XbaI (3651)
BMP7
HindIII (4946)
CMVp
pVAX1-BMP2/7- (6476 bp)

B

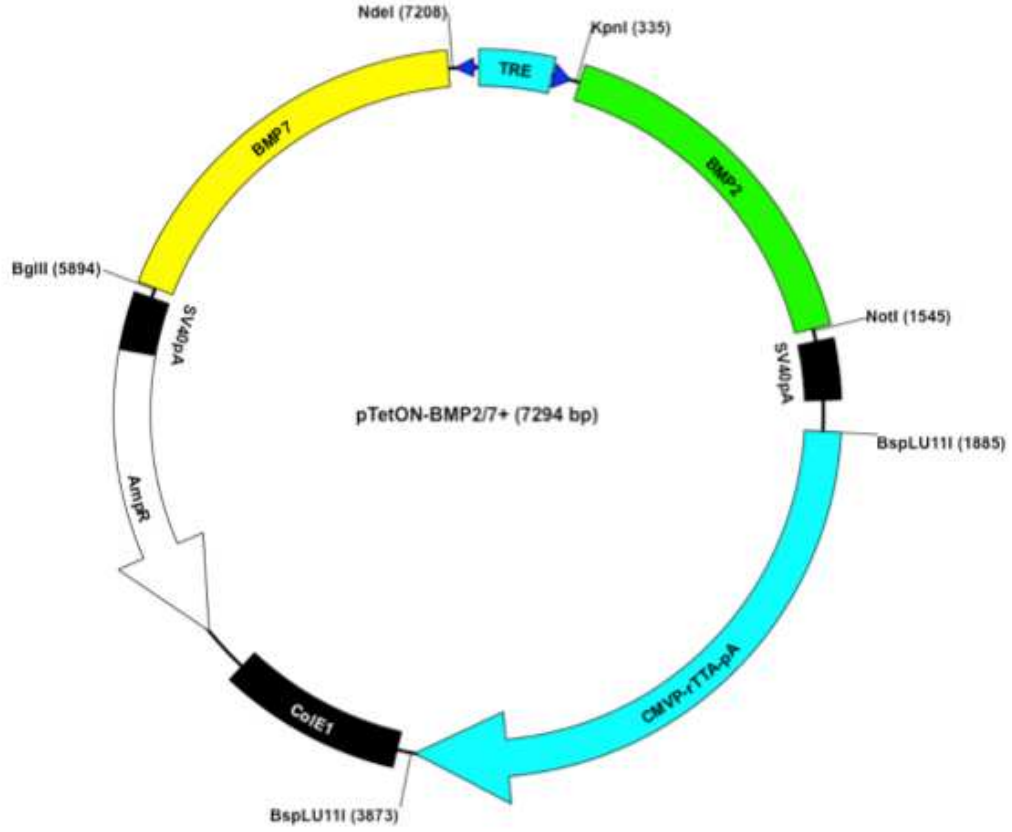
NdeI (7208)
KpnI (335)
TRE
BMP2
NotI (1545)
SV40pA
BspLU11I (1885)
CMVP-rTTA-pA
CoIE1
BspLU11I (3873)
AmpR
SV40pA
BglII (5894)
BMP7
pTetON-BMP2/7+ (7294 bp)

Supplementary Information: Constitutive and Inducible BMP2/7 Co-Expression Plasmids

Constitutive system pVAX1-BMP2/7- (A): Dual constitutive CMV-promoter cassette based BMP2/7 co- expression plasmid with BMP cassettes in divergent orientation. BMP2 cDNA sequence (green), BMP7 cDNA (sequence (yellow), CMV-promoter (CMVp, black arrow), bovine growth hormone poly-adenylation signal (BGHpA, black box), pUC origin of replication (pUC ori, black box), Kanamycine resistance gene (KanR, white arrow).